Development of a Field Technique for Measuring Fresh Water Ice Density

N.D. MULHERIN, M.G. FERRICK, P.B. WEYRICK,
N.M. PERRON AND S. HUNNEWELL
U.S. Army Cold Regions Research and Engineering Laboratory
72 Lyme Road
Hanover, New Hampshire 03755-1290, U.S.A.

ABSTRACT

Warming and subsequent deterioration of river and lake ice during the spring thaw cause dramatic changes in its material properties. This paper investigates whether the ice porosity or, alternatively, the drained density can be quantified in the field. The accuracy and precision of field mass/volume measurement of cylindrical ice cores were obtained by comparing with mass/volume measurements made on the same samples after careful machining in the laboratory. In addition, some of the ice samples were later analyzed using a submersion weighing method that is highly accurate for bubble-free ice, and these results were compared with the two mass/volume methods. This preliminary analysis indicates that the field method may be adequate for characterizing both the spatial variability of ice density and the temporal changes in this density distribution.

INTRODUCTION

Dramatic structural changes occur during the spring thaw as ice warms to its melting point and deterioration develops. The ice weakens rapidly as the grain boundaries melt and the individual crystals become more visually distinct. As decay progresses, the grain boundaries within the ice become liquid-filled pores that can eventually develop into relatively large intergrain voids. This decay represents a substantial increase in ice porosity and therefore a decrease in density when the ice is allowed to drain. Ice density, or porosity, is an important parameter in a wide range of problems and processes. Several studies have related changes in the mechanical properties of ice to changes in porosity. The usual assumption made for sea ice is that the brine volume is sufficiently greater than the air volume that the latter can be neglected. It follows that brine volume and porosity are virtually equivalent parameters. Vaudrey (1977) presented regression equations that relate tensile, flexural, compressive strength and elastic modulus data for sea ice to the square root of the brine volume. Weeks and Ackley (1982) presented geometric arguments that support a decrease in sea ice strength and elastic modulus with increasing brine volume. Ashton (1985) also used a geometric argument for grain boundary melting during deterioration of freshwater ice that relates decreasing strength to the square root of the porosity. Prowse et al. (1990) conducted in-situ beam tests and measured solar radiation during springtime thawing to relate calculated freshwater ice porosity to flexural strength.

We propose that ice density may be measurable in the field with an accuracy that is adequate to monitor small but significant temporal changes. The field method must allow many samples to be analyzed in a short time to obtain the density distribution representing the ice sheet at a given river location, and to resolve vertical density differences through the sheet. Our field method of choice was mass and volume measurement of right cylindrical ice cores. We recognize that water drainage from a sample will never be perfectly complete. Some water remains trapped within pores that are isolated from the exterior surface. Even with an abundance of pore networks, their geometry and adhesion of water to the pore walls work against complete drainage. Undrained water would be weighed as ice, resulting in a greater than actual density calculation. However, the importance of isolated meltwater was minimized in this study

due to our samples having a small radius and volume-to-surface ratio. The error introduced by network pore water retention depends on the pore size distribution and is potentially correctable.

The density values measured in the field were compared with similar measurements made in the laboratory after refreezing, end-milling and machine-lathing the same samples into uniform right circular cylinders with a smooth surface finish. These laboratory measurements represent the highest possible accuracy and precision that we could attain with the method. In addition, the densities of selected samples were determined using a laboratory submersion weighing method that is highly accurate and precise for bubble-free ice. Since one of the samples analyzed by submersion was nearly bubble-free, it served as a standard by which to compare the accuracy of the mass/volume meeasurements. This paper discusses our field and laboratory density measurement methods and compares the data obtained from each.

ICE CHARACTERIZATION AND FIELD PROCEDURE

The 62 ice samples for this study were cored from the Connecticut River at Hanover, New Hampshire, on three days during March 1991. The ice sheet ranged in thickness from 45 to 60 cm, which is a typical late winter range for rivers in this area. The in-situ ice temperature measured approximately 10 cm below the surface was 0.0°C on each of these days and the air temperature was approximately 5°C. The only apparent change in the ice sheet over the time period was in the extent of ice deterioration. Grain boundary melt was not observed on 1 March, was minor and localized on 7 March, and had developed some pore networks by 19 March.

The mode of ice growth in rivers is dominated by the hydraulic conditions. The 1991 coring location was in the backwater of the Wilder Dam at a section with a mean depth of 10 m and width of 150 m. During maximum turbine discharge, the mean flow velocity through the reach is 0.19 m/s. Matousek (1984) presented an empirical plot that related congelation, skim and frazil ice growth regimes in a river primarily to the flow velocity. This plot indicates that congelation growth is the dominant mode of ice formation at flow velocities below 0.2 m/s.

Gow (1986) discussed orientation textures of ice sheets on small lakes with negligible currents and turbulence at the time of formation. He observed and described congelation ice of types S1 and S2, depending on the seeding conditions at the time of formation. Thin sections were obtained for seven of our river ice cores, and c-axis orientation measurements were performed on the Rigsby universal stage (Langway 1958). The orientation data for each sample was analyzed using the methods of Ferrick and Claffey (1992). The average deviation from a vertical c-axis for all samples was less than 8°, indicating that the sheet was congelation ice of S1 type. The formation and growth processes at this river location were identical to those in small lakes. The density measurements discussed in this paper correspond to S1 ice and overlying snow ice. We have obtained similar data for a predominantly frazil ice cover at another location on the Connecticut River that will be discussed in a future paper.

At the sampling site, we obtained vertical cores with uniform diameters of about 10.5 cm using a precision core barrel powered by a light-weight gasoline engine. The cores were cut into right circular cylinders approximately 20 cm long using an electric miter saw and then allowed to drain while shaded from direct sunlight. The length and diameter of each sample were measured with calipers at least 20 times to the nearest 0.003 cm with their mean values and standard deviations (SD) being retained. After draining for at least 20 min, the samples were towel-dried and weighed to the nearest 0.1 g on an electronic balance that was fully enclosed in a Plexiglas windscreen. The balance was checked with a precision standard weight prior to each measurement and recalibrated if in error by more than 0.1 g. Drainage time is limited by melting that adversely reduces the uniformity of the core dimensions. The mass/volume density of each sample was calculated using the mean length and diameter. After field measurement, the samples were placed in core tubes and buried in snow until transported to the laboratory. In the laboratory coldroom, they were immediately removed from the core tubes, allowed to refreeze, sealed in individual plastic bags and stored at –20°C to await further analysis.

LABORATORY PROCEDURE

All 62 field samples were reanalyzed between 18 July and 27 August 1991 in a laboratory coldroom set at –10°C. They were carefully turned down on a lathe to produce slightly smaller cylinders with a smooth surface and a uniform diameter. The cores were also trimmed on a milling machine to obtain smooth and parallel end surfaces. The diameters and lengths were then remeasured with the same equipment and technique that were used in the field. Their masses, how-

ever, were obtained using an electronic balance with an additional digit of accuracy. It was expected that these laboratory procedural improvements would minimize measurement error and provide an upper bound on the accuracy and precision attainable using the field technique. Minimal measurement error would allow the laboratory data to be used as a standard to determine the accuracy of both the individual and population field measurements.

A selection of six samples were chosen for density analysis by laboratory fluid submersion (Butkovich 1953) because its accuracy in density determination would establish upper bounds for the mass/volume measurements. This subset of samples covered nearly the full range of density and ice type present in the complete set. In this method, a sample is weighed in air and then weighed in a fluid of known density. If the ice, air and liquid temperatures are all assumed to be equal, the density of the ice, ρ_i is determined as

$$\rho_i = \frac{\rho_l W_a}{W_a - W_l} \quad (1)$$

where ρ_l = the density of the liquid (g/cm^3)
W_a = the weight of the ice sample in air (g)
W_l = the weight of the sample in liquid (g).

The liquid used for the submersion density work was water-saturated 2,2,4–trimethylpentane, also known as isooctane. Water is highly insoluble in it, only 0.006% at 20°C; its freezing point is –107.4°C, and it has a lower density than ice. It is also cleaner and easier to use than other fluids (e.g., kerosene) because it is highly volatile and evaporates quickly.

The density of isooctane was measured over the full range of temperatures to be expected during the submersion procedure. A hygrometer graduated to 0.0002 and a mercury thermometer readable to 0.05°C were used to verify the linear relationship between specific gravity and temperature of the isooctane, with a correlation coefficient of 0.996. The simplicity and accuracy of the temperature measurement was exploited to find the liquid density. Three laboratory-grown, bubble-free ice samples served as standards for the submersion procedure. Measurements were conducted six different times on these nine samples, with each set of submersion measurements taking 30 to 40 min. The coldroom fan was shut down during that time to eliminate air turbulence interfering with the balance. This caused a slight rise in the coldroom air temperature but never more than 1°C. The associated rise in liquid temperature was generally less than 0.5°C.

The electronic balance used for the fieldwork was also used for the submersion procedure. It was equipped with a weighing hook on its underside that allowed the weighing pan to be suspended on a wire through a hole in the tabletop. Under the table and directly beneath the balance was a Plexiglas tank containing isooctane. When the pan and sample were suspended in the tank, isooctane was added or withdrawn before weighing to ensure that the pan was always submerged to the same level. This allowed the constant buoyant force on the pan to be neglected in the calculations. The accuracy of the balance was checked with standard weights before and after each submersion series.

COMPARISON OF MEASUREMENT METHODS

The density of each sample in the subset was determined using all three methods. These samples are described as follows with the coring date indicated in the sample name as a three-digit prefix:

301-213	Nearly bubble-free, maximum density expected.
301-109	Top two-thirds bubbly and bottom third clear.
301-102	Completely bubbly.
307-208	Clear ice with some pore development, corresponding to the start of ice deterioration.
319-218	Some bubbles, pore network and small void development.
319-215	Some bubbles, pore network and large void development.

Figure 1 shows samples 301-213 and 301-102 as examples of highly variable structure. Both were cored on the same day but 213 was nearly bubble-free while 102 was opaque with fine bubbles. Sample 319-215, an example of a deteriorated specimen, is also shown in Figure 1.

Table 1 shows summary statistics for the density measurements. The repeatability and accuracy of the submersion technique is illustrated in the statistics for the bubble-free standards. The mean densities for these three samples were identical, 0.9181 g/cm^3 with a SD of 0.0004 or less. Bader (1964) calculated the density of single-crystal (bubble-free) ice as a function of temperature between 0° and –30°C assuming constant atmospheric pressure. Our measured values of 0.9181 g/cm^3 for the lab-grown, bubble-free standards at –10°C agree very well with Bader's theoreti-

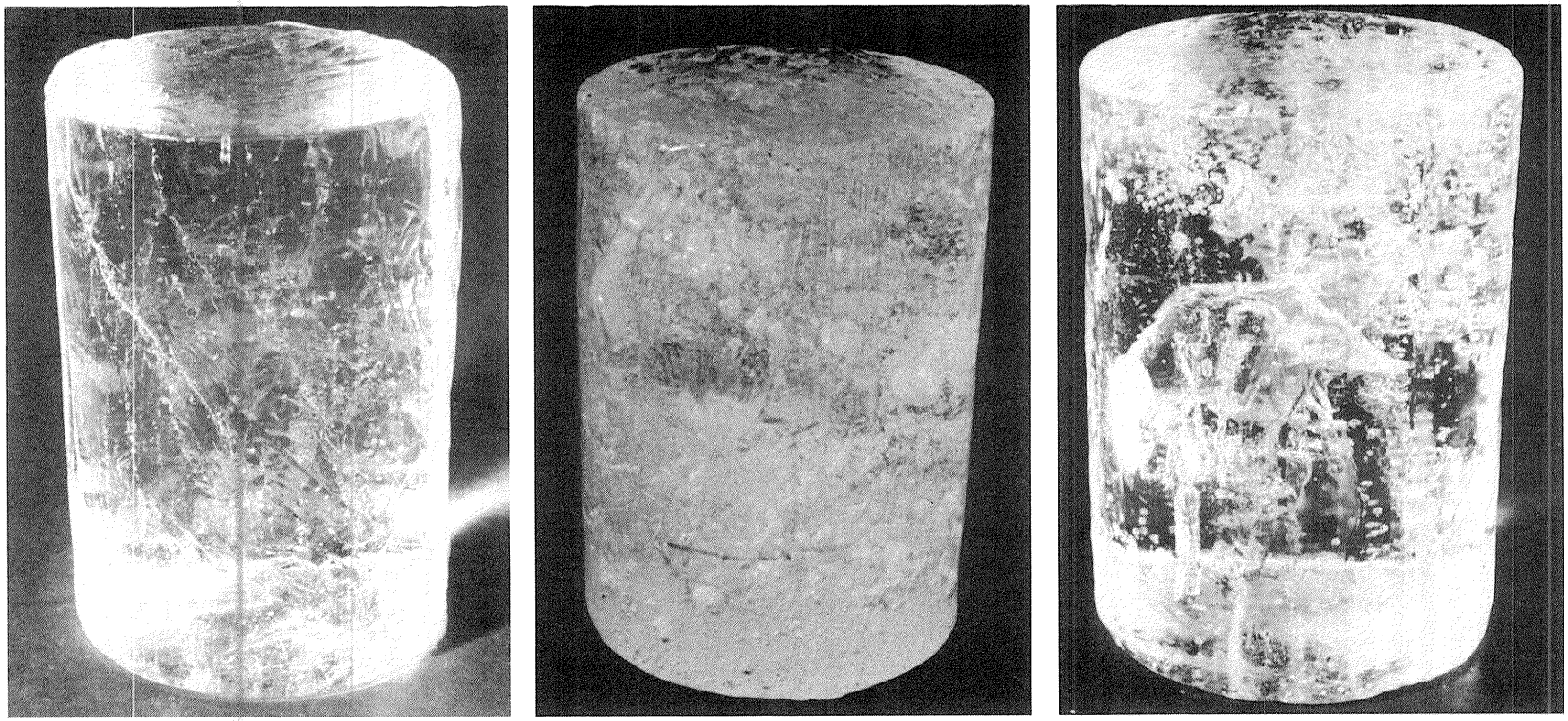

a. Sample 301-213. *b. Sample 301-102.* *c. Sample 319-215.*

Figure 1. Typical river ice samples that were analyzed for this study showing the range in structure from nearly bubble-free, to very bubbly, to relatively deteriorated.

Table 1. Field and laboratory ice density measurements for 6-sample subset and mean values for the full 62-sample set. The "+/–" value is the deviation from the mean density calculated using plus and minus one standard deviation of the ice core diameter and length.

	Laboratory Submersion				
River ice	*Density (g/cm³)*		*Bubble-free*	*Density (g/cm³)*	
Sample	*Mean*	*SD**	*ice standard*	*Mean*	*SD**
301-213	0.9179	0.0003	BF-1	0.9181	0.0004
301-109	0.9072	0.0004	BF-2	0.9181	0.0003
301-102	0.8914	0.0005	BF-3	0.9181	0.0004
307-208	0.9153	0.0004			
319-218	0.9056	0.0007	*Calculated from the six submersions		
319-215	0.9102	0.0004	performed on each sample.		
Mean	0.9079	0.0005			

	Field Mass/volume						
River Ice	*Diameter (cm)*		*Length (cm)*		*Weight*	*Density (g/cm³)*	
Sample	*Mean*	*SD*	*Mean*	*SD*	*(g)*	*Mean*	*+/–*
301-213	10.503	0.0231	17.574	0.0343	1385.7	0.9100	0.0058
301-109	10.474	0.0187	18.296	0.0095	1419.1	0.9002	0.0037
301-102	10.472	0.0180	16.990	0.0401	1293.9	0.8843	0.0051
307-208	10.450	0.0147	17.490	0.0255	1359.0	0.9059	0.0039
319-218	10.475	0.0109	17.930	0.0140	1382.0	0.8944	0.0026
319-215	10.475	0.0173	17.074	0.0109	1309.5	0.8900	0.0035
6-Sample Mean		0.0171		0.0224		0.8975	0.0041
62-Sample Mean		0.0149		0.0257		0.9044	0.0039

	Laboratory Mass/volume						
River Ice	*Diameter (cm)*		*Length (cm)*		*Weight*	*Density (g/cm³)*	
Sample	*Mean*	*SD*	*Mean*	*SD*	*(g)*	*Mean*	*+/–*
301-213	9.561	0.0021	13.898	0.0041	913.36	0.9154	0.0007
301-109	9.102	0.0016	13.296	0.0044	782.10	0.9040	0.0006
301-102	9.424	0.0031	13.261	0.0034	818.76	0.8851	0.0008
307-208	9.374	0.0028	13.611	0.0040	853.56	0.9087	0.0008
319-218	9.829	0.0027	15.391	0.0037	1038.23	0.8891	0.0007
319-215	9.719	0.0029	13.657	0.0042	899.46	0.8878	0.0008
6-Sample Mean		0.0025		0.0040		0.8984	0.0007
62-Sample Mean		0.0032		0.0041		0.9058	0.0009

cal value of 0.9179 g/cm^3, confirming the accuracy and precision of our experimental technique. The ice sample most similar in visual appearance to our bubble-free standards was 301-213, representing clear ice in an undeteriorated ice sheet. Its submersion density was expected and found to be the maximum value, 0.9179 ± 0.0003 g/cm^3. This result is both accurate and precise enough to gauge the accuracy of the mass/volume methods.

It is intuitive that the more porous the ice being analyzed, the less accurate its submersion density. Air bubbles and melt voids in the ice that are open to the surface fill with liquid when immersed, effectively reducing the sample volume. The net effect is higher-than-actual specimen density that consistently exceeded the mass/volume measurements for the six samples. Although accuracy decreases with increasing porosity, repeatability was relatively unaffected because the samples were submerged with the same orientation from trial to trial. The pores that are open to the surface allow varying degrees of liquid infiltration if the orientation is different in successive trials, which would translate to large scatter in the results. However, with careful alignment, the SD calculated from the six immersions performed on each sample was negligibly small.

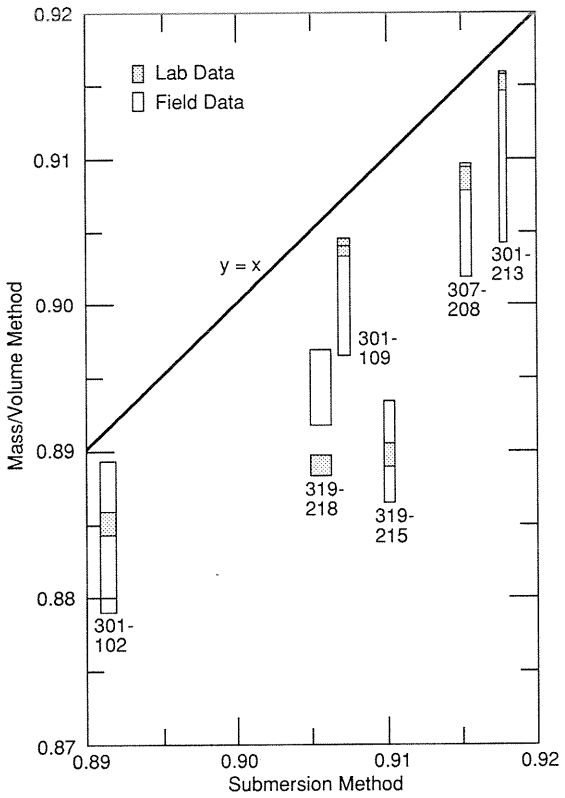

Figure 2. Comparison of the mean densities for the six samples analyzed by submersion with their means measured using the field and laboratory mass/volume methods. The dimensions of the plotted rectangle, both horizontally and vertically, correspond to the mean ± 1 SD of the measurements.

In the field, the SD of the diameter measurements for the six-sample subset ranged from a low value of 0.0109 cm to a high of 0.0231 cm. The same range for the length measurement was 0.0095 to 0.0401 cm. For each sample, a greater volume and a smaller volume were calculated by using the mean length and diameter plus and minus their respective SD. This produced a minimum-to-maximum density "range" for each sample that is twice the "+/–" value in Table 1. These ranges for the fieldwork were between 0.0051 and 0.0116 g/cm^3 and averaged 0.0082 g/cm^3.

In the laboratory, the diameter measurements were more precise on average by a factor of seven. One SD for the diameters averaged 0.0025 cm, as compared to 0.0171 cm for the field measurements. There was similar improvement in the length precision. One SD for the lengths averaged 0.0040 cm compared to 0.0224 cm for the field values. The corresponding minimum-to-maximum ranges for the laboratory work were less variable than the field values, ranging between 0.0012 and 0.0016 g/cm^3.

The minimum-to-maximum density ranges obtained via mass/volume are comparable to twice the SD for submersion. That is, the submersion range averaged 0.0009 g/cm^3, roughly two-thirds that of the lab mass/volume work and nine times less than that for the fieldwork.

The mean, minimum, and maximum densities obtained with each of the methods are compared in Figure 2. The vertical dimension of each box corresponds to the minimum-to-maximum density range of the mass/volume methods. The horizontal dimension shows the mean plus and minus the standard deviation for the submersion method. The boxes all fall below the line of perfect agreement. The most bubble-free river ice sample, 301-213, had a submersion density that differed the least from its mass/volume density. The more deteriorated samples had the largest density differences between the submersion and the mass/volume methods. The laboratory mass/volume density range was always smaller and generally contained within that for the field. The mass/volume densities for 301-218 agree to two decimal places even though there is no overlap between them.

From intact ice to the most deteriorated of our series, the lab mass/volume method gives a range in density for the six core samples of only 0.0303 g/cm^3. The same value for the field mass/volume method was 0.0257 g/cm^3 and the submersion method ranged over 0.0265 g/cm^3. Relatively small changes in ice density correspond to significant changes in the ice structure and properties. The absolute value of the difference between the field and laboratory mass/volume densities ranged from 0.0008 to 0.0054 g/cm^3, the lab density being greater than the field density for all samples except the two most deteriorated ones. The importance of this comparison is that the field densities agree with the laboratory results to two decimal places, which implies that we can identify small changes in ice density with the proposed field method when the length and diameter of the core are sufficiently uniform.

ANALYSIS OF COMPLETE DATA SET

The mass/volume density means and SD for the full 62-sample data set, presented in Table 1, closely match the corresponding values for the 6-sample subset, implying that the conclusions drawn from the subset also apply to the full set. The SD values for the full set of field and laboratory diameters and

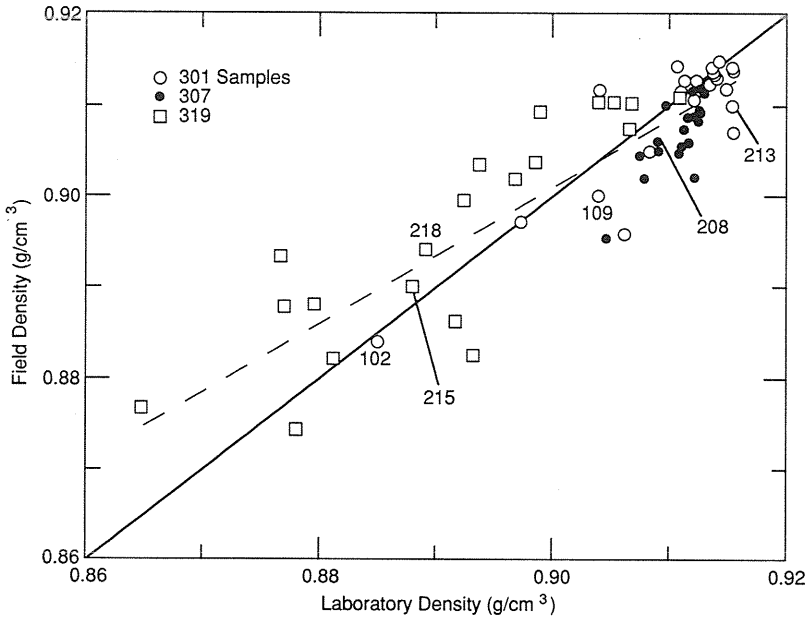

a. All samples. Numbered points indicate samples that were analyzed by submersion.

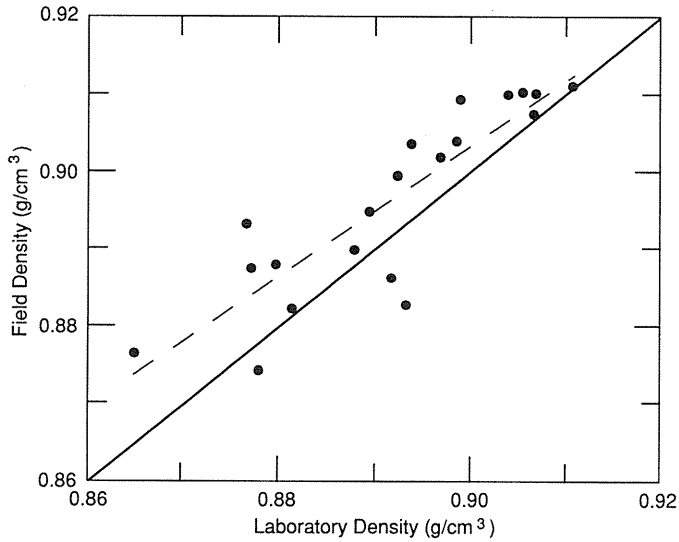

b. The 19 March data only.

Figure 3. Comparison of the mass/volume densities showing the least-squares line of best fit (dashed) relative to the line of perfect agreement (solid).

lengths were 0.0149 and 0.0032 cm, and 0.0257 and 0.0041 cm, respectively. The field and laboratory minimium-to-maximum density ranges for the full set were 0.0078 and 0.0018 g/cm^3. The precision improvement from the field to the lab in determining mean density was 4.3 times for the full data set and 5.9 times for the subset.

The mean laboratory and field densities for the full data set are plotted in Figure 3a and the six samples already discussed are labelled. The field-vs.-lab comparison for the 19 March data alone appears in 3b. The line of perfect agreement between field and lab values is shown relative to a least squares regression line of best fit in each plot. The line of

best fit was obtained with field density as the dependent variable, reflecting the larger measurement errors in the field. The correlation coefficient of the regression in Figure 3a is 0.885 and the mean distance of the data from that line is 0.0047 g/cm^3. On 1 and 7 March the mean laboratory density exceeded that in the field by 0.0025 g/cm^3. As a result of practice, the measurement precision of the lengths and diameters was best on 19 March. However, the mean field density on that date exceeded that in the laboratory by 0.0045 g/cm^3 (Fig. 3b). With increased precision, it is unlikely that a systematic measurement error was reversed and increased in magnitude. The samples continued to drain for about an hour after field measurement and before placement in the coldroom. The entire difference in mean density between the field and laboratory measurements can be explained by an average of only 7 g of additional water drainage from a 1390-g sample, the average mass for a 19 March field sample. If slow water drainage from small pore spaces is the primary reason for this difference, we would expect an increase in the volume of retained water as the number of pores increases with deterioration, at least in the early stages of deterioration. This hypothesis is supported by the data. Both regression fits show the trend toward larger variation between the field and lab densities with increasing porosity. Eventually, a maximum volume of retained water should be reached as pore size increases and the network becomes more extensive, but this is speculative and beyond the scope of our data.

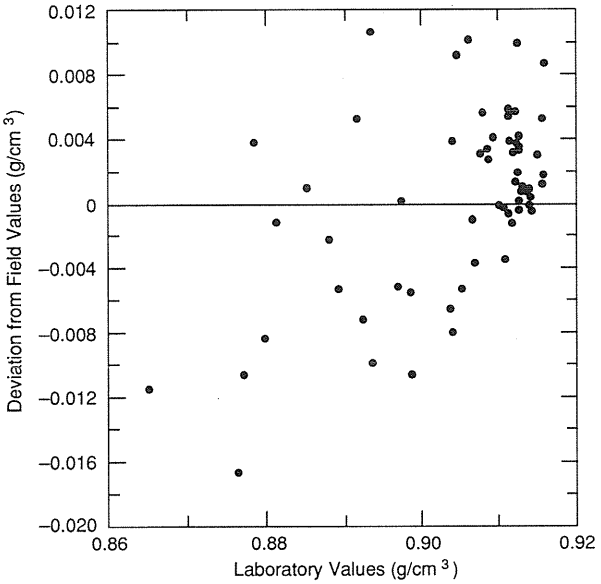

Figure 4. Residuals plot for the field density with laboratory mass/volume density. A trend is evident in the deviation moving from lower to higher ice density unless the four points in the lower left are disregarded.

The data presented in Figure 3a are replotted in Figure 4 with the density difference, laboratory minus field, as the ordinate. The mean distance of the

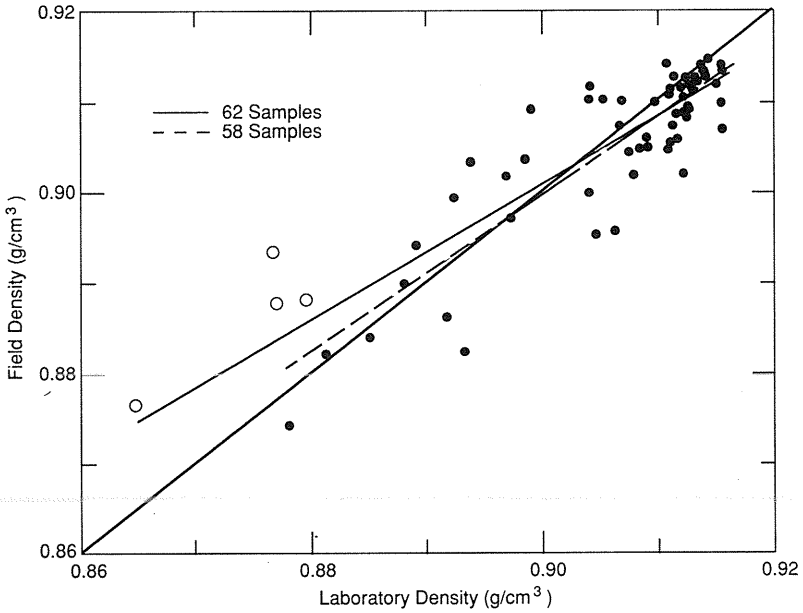

Figure 5. Comparison of the mass/volume densities showing the influence of the four points indicated. The original, 62-sample- and the new, 58-sample-least-squares lines of best fit are shown relative to the line of perfect agreement.

data from the zero line, the line of perfect agreement, is 0.0056 g/cm^3, slightly greater than the 0.0047-g/cm^3 distance from the line of best fit. The pore-water-retention trend can also be noted in these residuals. This figure makes more apparent the effect that the four data points in the lower leftmost corner have on the regression analysis. The trend that we just described goes away if these four points are discounted for any reason. This hypothetical, 58-sample data set has an average deviation from the perfect-fit line of only 0.0045 g/cm^3. Stated in another way, without these four points, the density distribution we obtained in the field was extremely close to that obtained in the laboratory. Figure 5 shows both the original regression fit and a new fit that discounts the four points. The effect of the four points in question have on the data raises questions. Additional data are needed in the lower density range to more firmly establish a relationship between the measurement techniques.

As individual points, the field and laboratory data appear to differ significantly. However, there is agreement when the field and laboratory data sets as a whole are compared. The overall mean of both data sets is 0.904 g/cm^3, with a field SD of 0.010 and a corresponding laboratory value of 0.012. Also, the ranges of the data are very similar: 0.874–0.915 for the field and 0.865–0.916 for the laboratory. The discrepancy in the minimum values is, again, due mainly to the four data points discussed earlier. Without those four points, the minimums converge to 0.874 for field and 0.878 for the lab and both SD reduce to 0.009. With the mean, SD, and extremes in close agreement, the distributions representing the field and laboratory data sets must be very similar. Given the relatively small measurement error, the variation seen in the laboratory densities was due mainly to actual variability of the density in time and space. Our individual field measurements contained significant error but the distribution representing the field data almost perfectly captured the mean density and its actual variability.

CONCLUSIONS

These experiments have provided quantitative information on the accuracy and precision of three methods for measuring ice density. The submersion method was very accurate and repeatable for bubble-free ice and was intended to provide an accuracy check for the two mass/volume methods. Although the repeatability was nearly unaffected, submersion density is increasingly less accurate for more highly deteriorated ice due to liquid-filling of voids and pores that are connected with the surface. The submersion procedure always provides an upper bound for the density.

The laboratory mass/volume measurements were performed under ideal conditions and provided an absolute limit on the accuracy and precision of the method. The environment and sample geometry are more highly controlled in the laboratory, producing better results than were achieved in the field by a factor of approximately six. The laboratory mass/volume method was sufficiently sensitive to provide an accurate representation of the ice cover density variability.

The field method is simple to perform but results are subject to the skill and experience of the personnel involved. Large improvements were gained with a small amount of practice. Field results improve with sample precision and so samples with large SD in length and diameter should be rejected in favor of more uniform samples. In the case of deteriorated ice, complete water drainage prior to measurement can never be fully accomplished due to isolated pore spaces and pore water retention. However, the sample size and shape minimized the isolated meltwater. Additional data and analysis can potentially quantify and correct field measurements for pore water retention. The field method did not provide consistently accurate individual measurements but it may be used to characterize the distribution of ice density when a large number of samples are taken. Though more study is needed, these results indicate that a mass/volume field technique for defining the density distribution of an ice sheet is attainable.

REFERENCES

Ashton, G.D.(1985) Deterioration of floating ice covers. *Journal of Energy Resources Technology,* **107**: 177–182.

Bader, H. (1964) Density of ice as a function of temperature and stress. USA Cold Regions Research and Engineering Laboratory, Special Report 64.

Butkovich, T.R. (1953) Density of single crystals of ice from a temperate glacier. USA Snow, Ice and Permafrost Research Establishment, SIPRE Research Paper 7.

Ferrick, M.G. and K.J. Claffey (1992) Vector analysis of ice fabric data. USA Cold Regions Research and Engineering Laboratory, CRREL Report 92-1.

Gow, A.J. (1986) Orientation textures in ice sheets of quietly frozen lakes. *Journal of Crystal Growth*, **74**: 247–258.

Langway, C.C., Jr. (1958) Ice fabrics and the universal stage. USA Snow, Ice and Permafrost Research Establishment, Technical Report 62.
Matousek, V. (1984) Types of ice run and conditions for their formation. *IAHR Ice Symposium 1984, Hamburg*, vol.1, pp. 315–327.
Prowse, T.D., M.N. Demuth, H.A.M. Chew (1990) Changes in flexural strength of ice under radiation decay. *Nordic Hydrology*, **21**: 341–354.
Vaudrey, K.D. (1977) Ice engineering study of related properties of floating ice sheets and summary of elastic and viscoelastic analysis. Civil Engineering Laboratory, Naval Construction Battalion Center, Port Hueneme, California, Report TR 860.
Weeks, W.F. and S.F. Ackley (1982) The growth, structure and properties of sea ice. USA Cold Regions Research and Engineering Laboratory, CRREL Monograph 82-1.